Electronic Supplementary Material (ESI) for Analyst.
This journal is © The Royal Society of Chemistry 2020

Electronic Supplementary Information

Ligand structure and charge state-dependent separation of monolayer protected Au_{25} clusters using non-aqueous reversed-phase HPLC

Korath Shivan Sugi,[a] Shridevi Bhat,[a] Abhijit Nag,[a] Ganesan Paramasivam,[a] Ananthu Mahendranath,[a,b] and Thalappil Pradeep*[a]

[a] *DST Unit of Nanoscience (DST UNS) and Thematic Unit of Excellence (TUE), Department of Chemistry, Indian Institute of Technology Madras, Chennai 600 036, India*

[b] *Department of Metallurgical and Materials Engineering, Indian Institute of Technology Madras, Chennai 600036, India.*

**E-mail: pradeep@iitm.ac.in*

Table of contents

SL. No.	Description	Page No.
	Calculation of selectivity (α)	3
	Computational methods	3
Fig. S1	Schematic representation of functionalized silica beads of reversed-phase columns	5
Fig. S2	Negative ion MALDI MS of cluster I, II, and III.	5
Fig. S3	Linear gradient program used for the separation	6
Fig. S4	Flow rate vs. eluent volume required in linear gradient [10] program	6
Fig. S5	Online UV-vis spectra of cluster I in C_{18} column with different flow rates	7
Fig. S6	Online UV-vis spectra of cluster II in C_{18} column with different flow rates	8
Fig. S7	Online UV-vis spectra of cluster III in C_{18} column with different flow rates	9
Fig. S8	Variation of peak width of half maxima at different	10

	flow rates of cluster I, II, and III in C_{18} column	
Fig. S9	Chromatograms of cluster a) I, b) II, and c) III at different flow rates in C_8 column	10
Fig. S10	Online UV-vis spectra of cluster I, II, and III in C_8 column with different flow rates	11
Fig. S11	Variation of peak width of half maxima at different flow rates of cluster I, II, and III in C_8 column	12
Fig. S12	Online UV-vis spectra of cluster I and II in a phenylhexyl column with different flow rates	12
Fig. S13	Variation of peak width of half maxima at different flow rates of cluster I, II, and III in phenylhexyl column	13
Table S1	Fitting parameters for the exponential fits	14
Fig. S14	Online UV-vis spectra of cluster IIIa, III, and mixture of both eluted in phenylhexyl column with 1.0 mL/min flow rate	15
Fig. S15	The energy minimum structures of octadecyl silyl functionality docked with cluster I, II, and III	15
Fig. S16	The energy minimum structures of octyl silyl functionality docked with cluster I, II, and III	16
Fig. S17	Concentration-dependent chromatograms of cluster III in the phenylhexyl column at 1.0 mL/min flow rate	16
Fig. S18	Peak area vs. concentration of cluster III in the phenylhexyl column at 1mL/min flow rate	17

Calculation of selectivity (α)

The selectivity (α) of the method is estimated using equation (1).

$$\alpha = \frac{K_2}{K_1} = \frac{t_{R2} - t_0}{t_{R1} - t_0} \qquad (1)$$

Here, K = retention factor of the separation

t_R = retention time of the peak

t_0 = dead time

Computational methods

DFT calculations

The structures of Au_{25} cluster protected with different thiols such as dodecanethiol (DDT) and octanethiol (OT) were built from the crystal structure of $Au_{25}(PET)_{18}$ cluster by replacing the phenylethanethiol (PET) ligands. All the geometries were optimized using density functional theory (DFT) with projector augmented waves (PAW) as implemented in the GPAW software package.[1] The atomic PAW setup was used as Au($5d^{10}6s^1$), S($3s^23p^4$), C($2s^22p^2$) and H($1s^1$), with scalar-relativistic effects included for Au. Further, these atomic orbitals were described by the DZP (double zeta plus polarization) basis set with the Perdew-Burke-Ernzerhof (PBE) exchange-correlation functional[2] in LCAO mode[3] to effectively include the interactions in the considered clusters. The geometries were relaxed with a grid spacing of 0.2 Å, and the convergence was set to minimize the residual forces without any symmetry constraints by 0.05 eV/Å.

Molecular docking calculations

Molecular docking studies were performed using AutoDock4.2 and its associated tools.[4] DFT-optimized geometries of clusters I, II, and III were used for the study. The different columns were computationally modeled by constructing a SiO_2 surface of ~ 5 nm by cutting out from

its crystal structure,[5] and the column functionalities such as octadecyl silyl, octyl silyl, and phenylhexyl silyl were attached to the silicon atoms on the SiO_2 surface. All the structures were built using Avogadro software package.[6] We used the cluster as "ligand" and stationary phase as "receptor". Receptor grids were generated using 126 × 126 × 126 grid points in XYZ, with a grid spacing of 0.375 Å, and map types were created using AutoGrid-4.2. The grid parameter file (.gpf) was saved using MGL Tools-1.4.6.50. The docking parameter files (.dpf) were generated using MGLTools-1.4.6.50. The results of AutoDock generated an output file (.dlg), and the generated conformers were scored and ranked as per the interaction energy. Ten lowest-energy conformers were obtained. We used the Lamarckian genetic algorithm for the output file using MGLTools-1.4.6.

Supplementary information 1

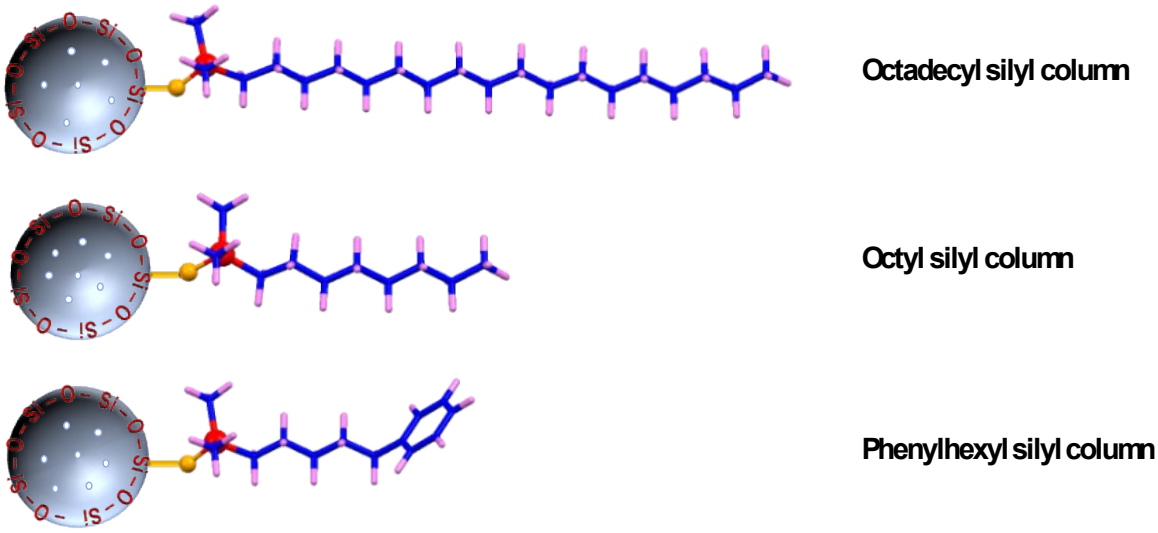

Fig. S1 Schematic representation of three different silica beads of reversed-phase HPLC columns. Color labels: blue, C; pink, H; red, Si; yellow, O.

Supplementary information 2

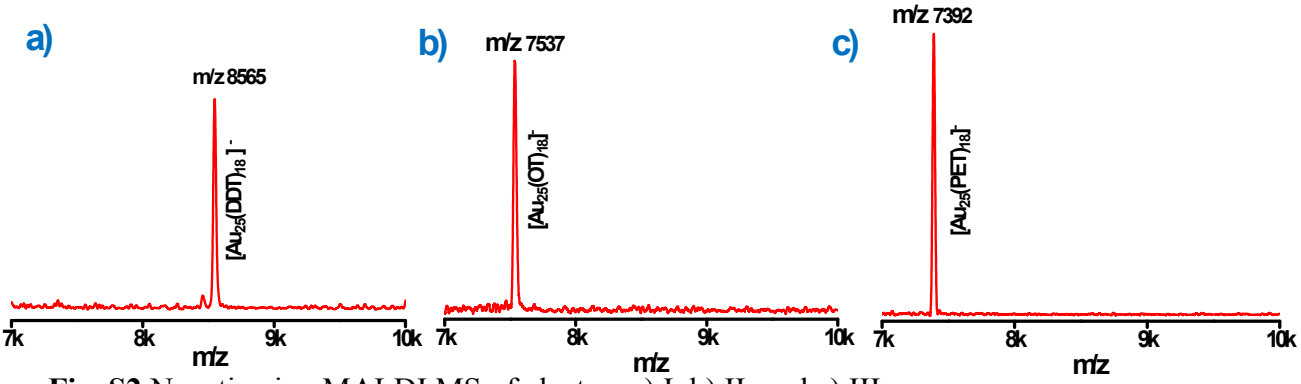

Fig. S2 Negative ion MALDI MS of clusters a) I, b) II, and c) III.

Supplementary information 3

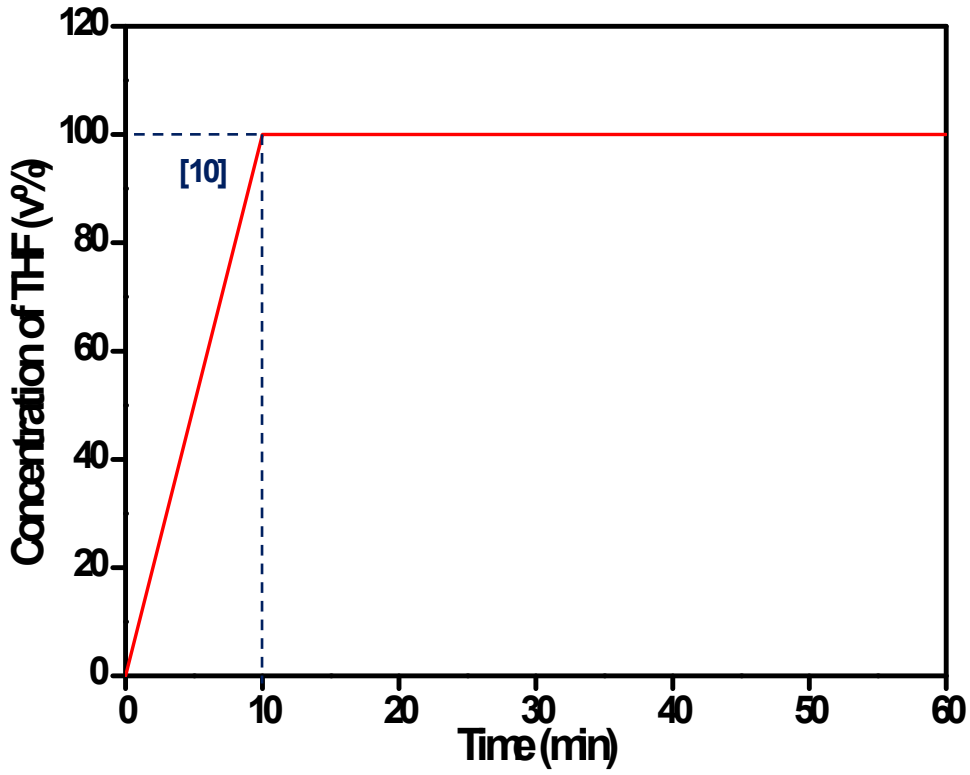

Fig. S3 Linear gradient program used for the separation of clusters. The label (e.g., [10]) indicates the time (in minutes) taken to replace the mobile phase fully with THF.

Supplementary information 4

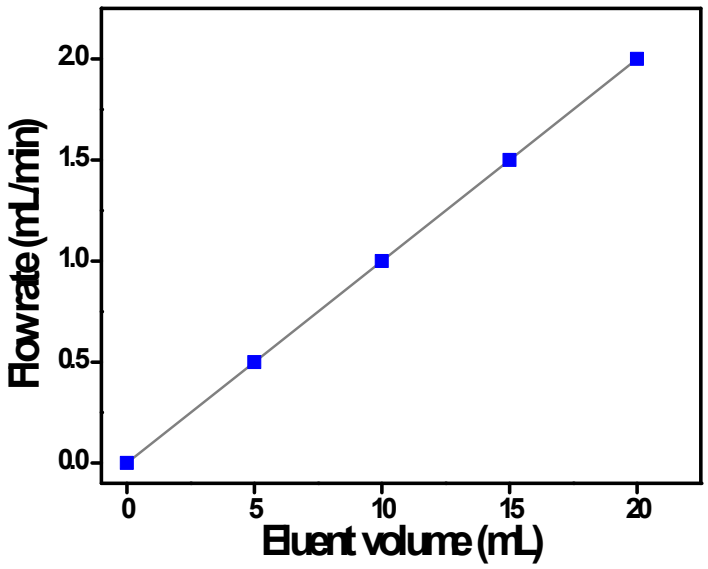

Fig. S4 Eluent volume required to replace 100% MeOH to 100% THF in a linear gradient [10] program with varying flow rate.

Supplementary information 5

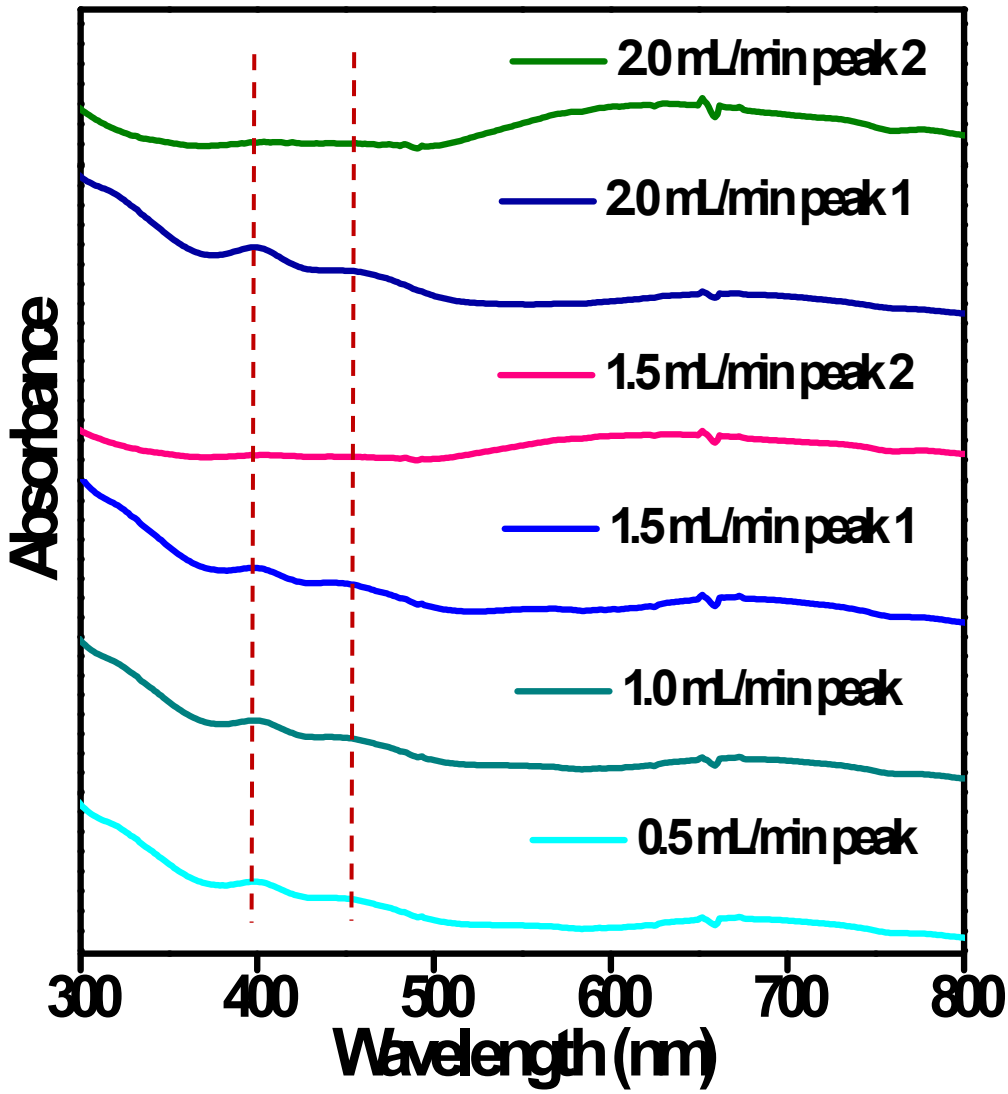

Fig. S5 Online UV-vis spectra of cluster I in C_{18} column at different flow rates, extracted at 400 nm wavelength obtained by PDA detector.

Supplementary information 6

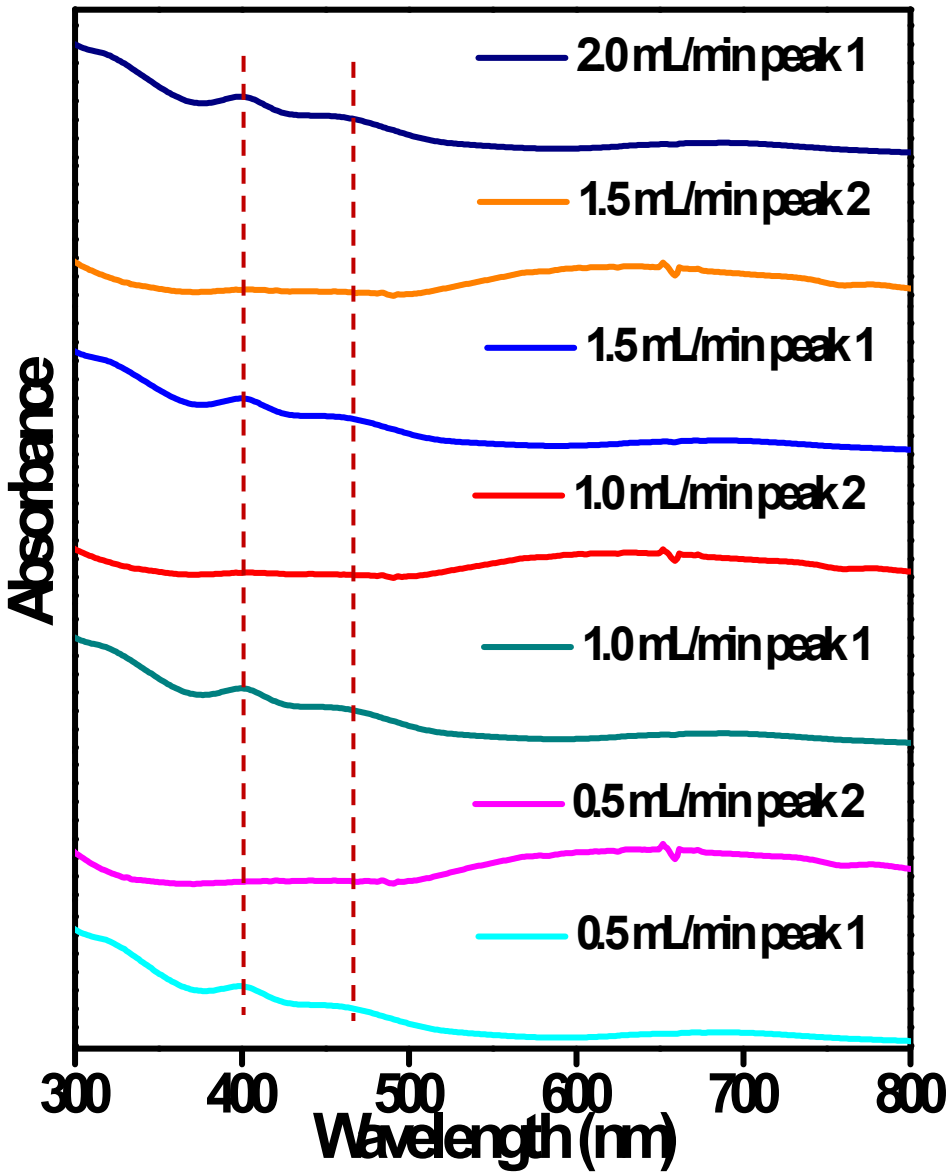

Fig. S6 Online UV-vis spectra of cluster II in C_{18} column at different flow rates, extracted at 400 nm wavelength obtained by PDA detector.

Supplementary information 7

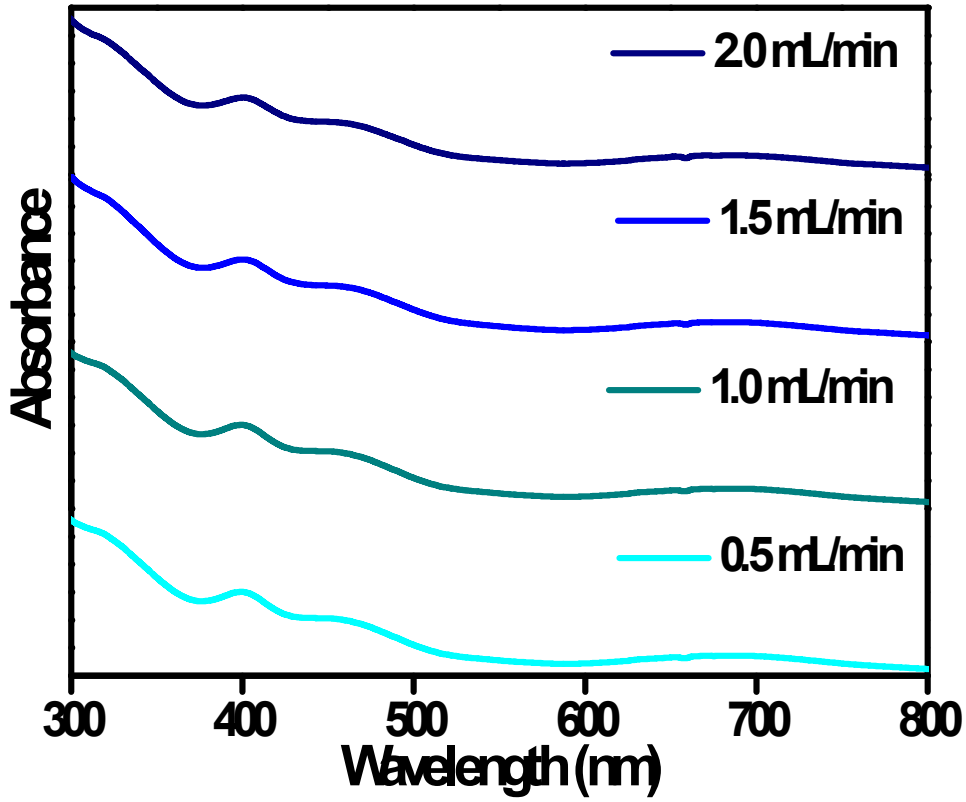

Fig. S7 Online UV-vis spectra of cluster III in C_{18} column at different flow rates, extracted at 400 nm wavelength obtained by PDA detector.

Supplementary information 8

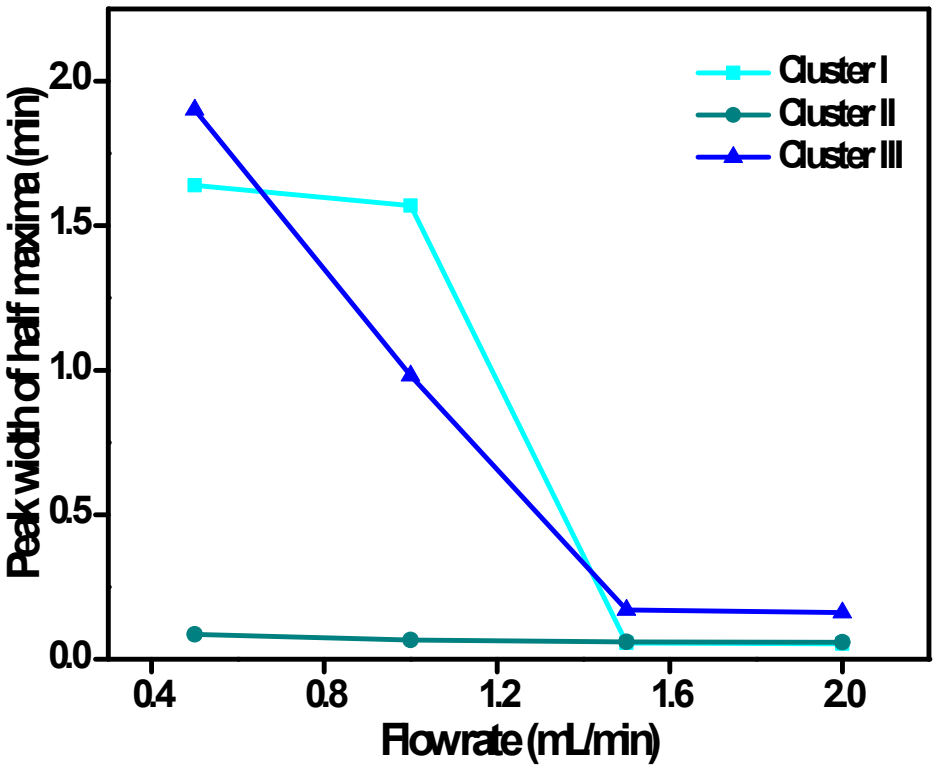

Fig. S8 Variation of peak width of half maxima with different flow rates of cluster I, II, and III in C_{18} column.

Supplementary information 9

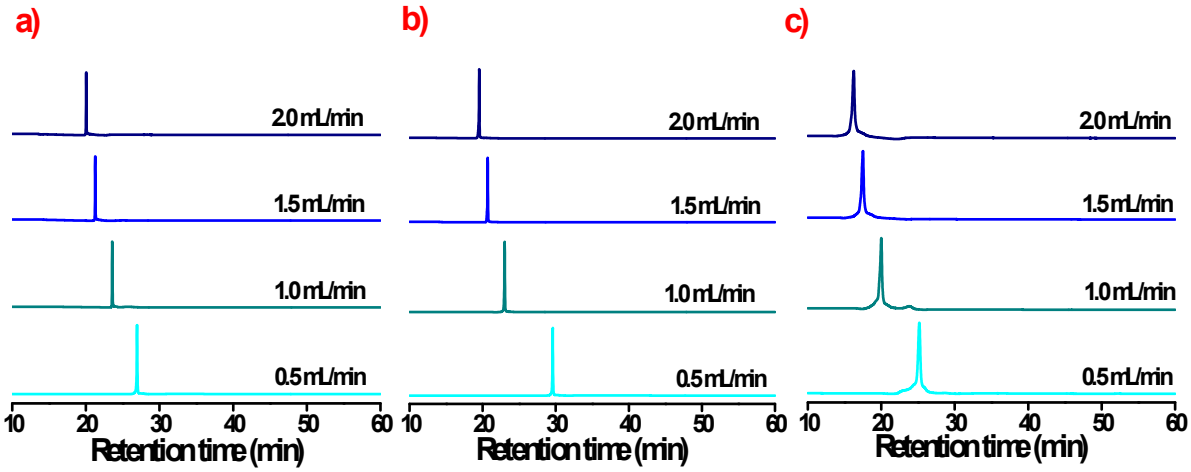

Fig. S9 Chromatograms of cluster a) I, b) II, and c) III at different flow rates in C_8 column.

Supplementary information 10

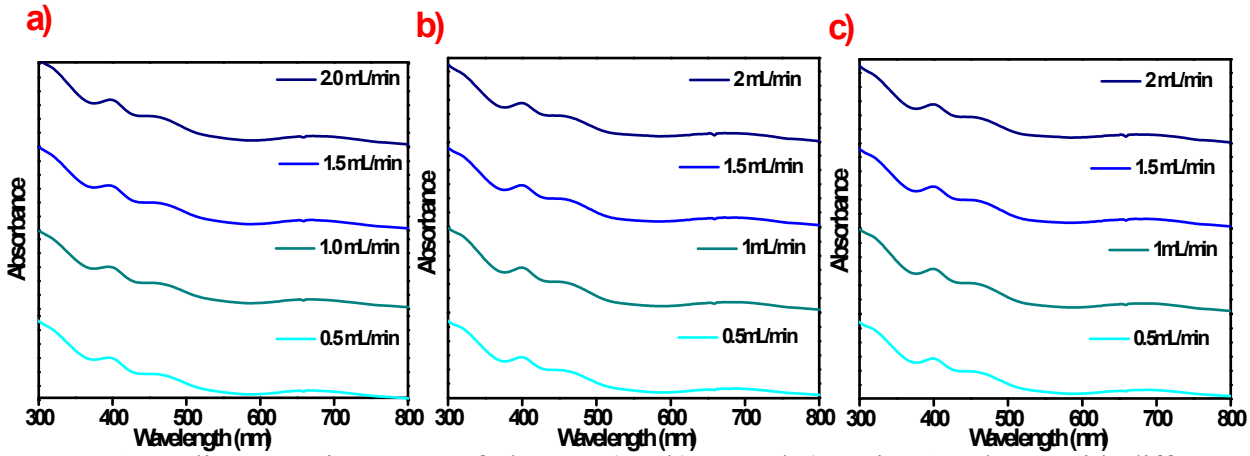

Fig. S10 Online UV-vis spectra of clusters a) I, b) II, and c) III in C_8 column with different flow rate obtained by PDA detector.

Supplementary information 11

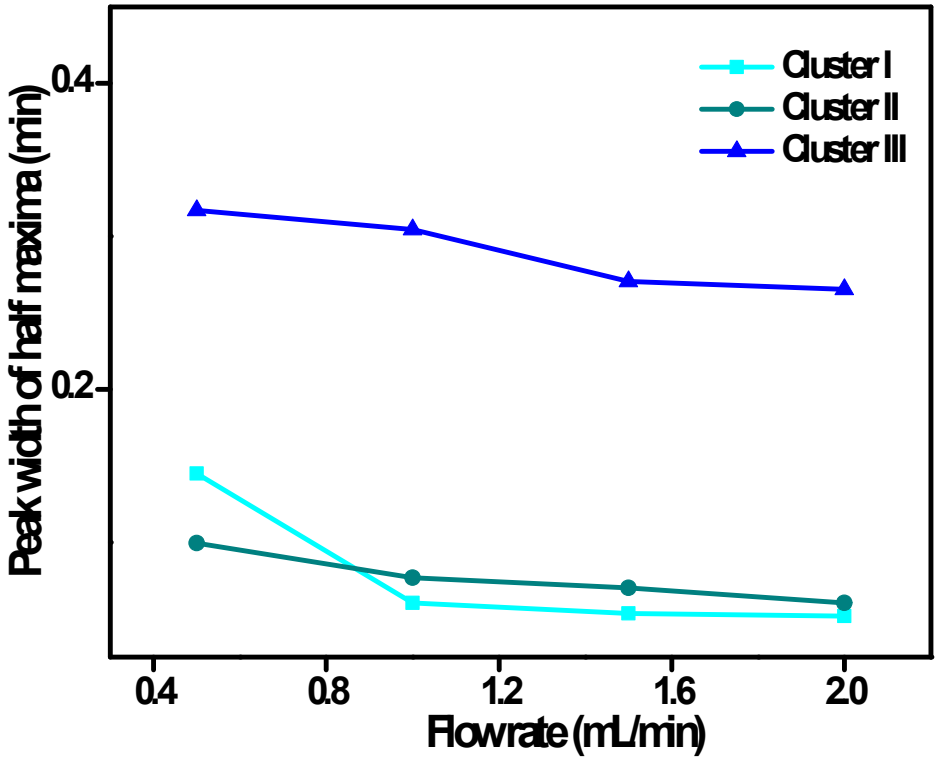

Fig. S11 Variation of peak width half maxima with different flow rates of cluster I, II, and III in C_8 column.

Supplementary information 12

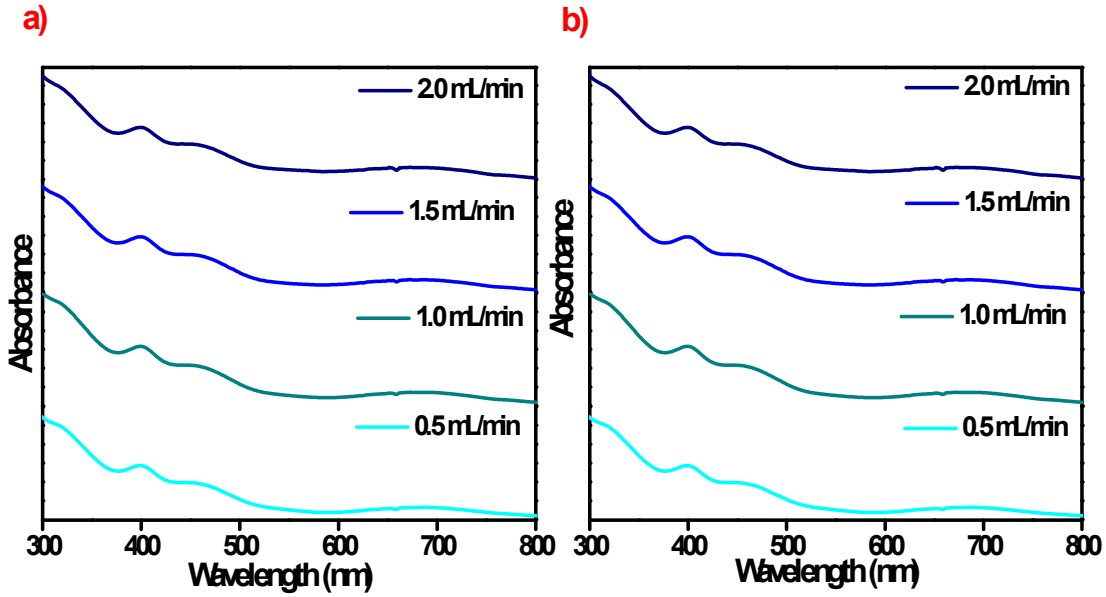

Fig.S12 a) and b) are the online UV-vis spectra of cluster I and II in a phenylhexyl column with different flow rates obtained by PDA detector.

Supplementary information 13

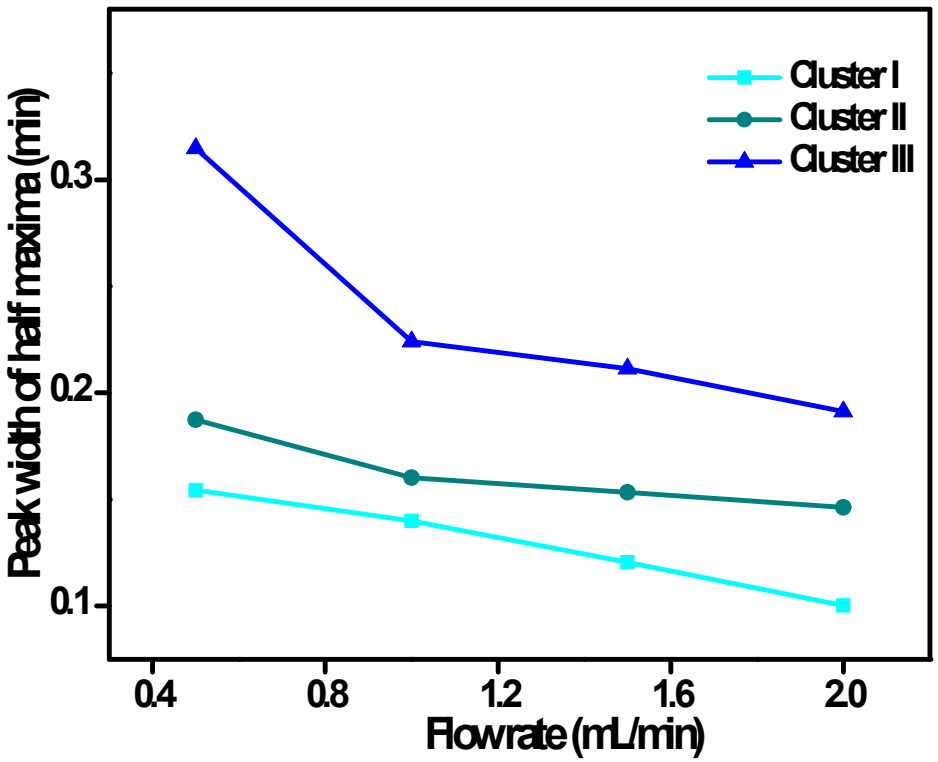

Fig. S13 Variation of peak width of half maxima with different flow rates of cluster I, II, and III in the phenylhexyl column.

Table S1 Fitting parameters for the exponential fits shown in Figure 7.

The fitting function has the form $t_R = A*(\exp(-x/b) + c$ where 'x' is flow rate in mL/min

Column	Cluster	A (in min)	b	c	R^2
C_{18}	$Au_{25}(DDT)_{18}$	28.136	0.687	18.74	0.992
C_{18}	$Au_{25}(OT)_{18}$	26.055	1.407	11.013	0.993
C_{18}	$Au_{25}(PET)_{18}$	37.033	0.951	12.380	0.991
C_8	$Au_{25}(DDT)_{18}$	28.680	0.515	19.530	0.997
C_8	$Au_{25}(OT)_{18}$	27.498	0.523	18.990	0.998
C_8	$Au_{25}(PET)_{18}$	26.914	0.559	15.55	0.998
Phenylhexyl	$Au_{25}(DDT)_{18}$	20.980	0.520	17.328	0.998
Phenylhexyl	$Au_{25}(OT)_{18}$	22.960	0.5118	16.815	0.998
Phenylhexyl	$Au_{25}(PET)_{18}$	22.151	0.545	16.597	0.997

Supplementary information 14

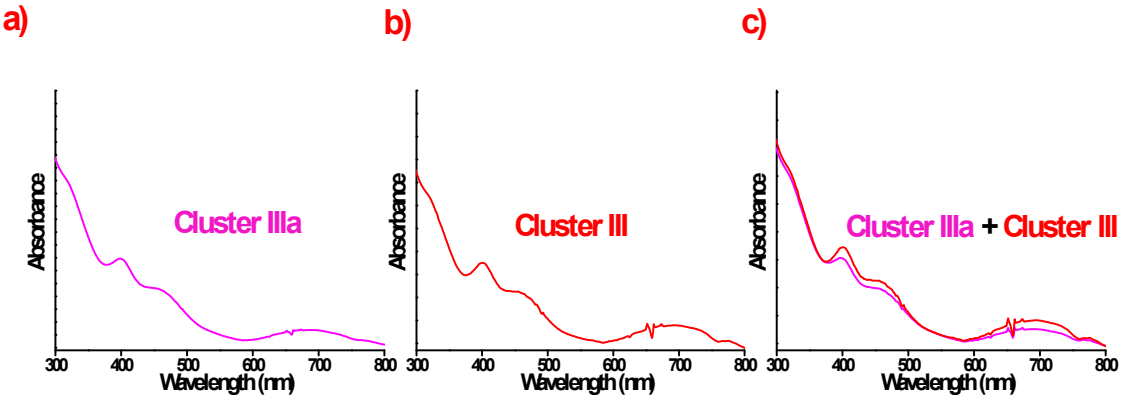

Fig.S14 a), b), and c) are the online UV-vis spectra of cluster IIIa, III, and mixture of both eluted in phenylhexyl column with 1.0 mL/min flow rate obtained by PDA detector.

Supplementary information 15

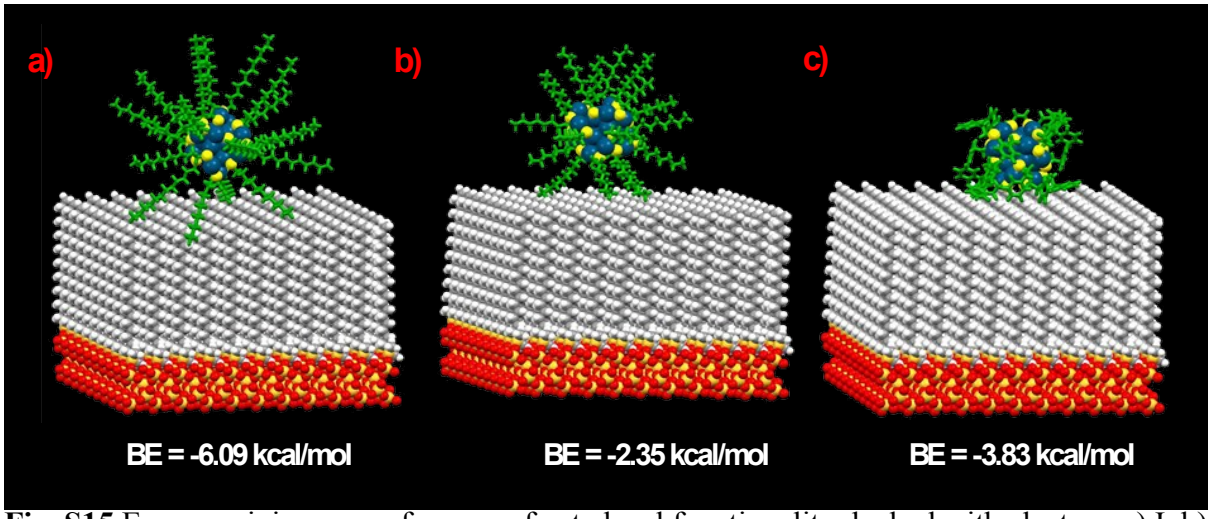

Fig. S15 Energy minimum conformers of octadecyl functionality docked with clusters; a) I, b) II, and c) III. Color labels: golden yellow, Si; red, O; grey, C; white, H; teal, Au; yellow, S; green, DDT, OT, and PET ligands.

Supplementary information 16

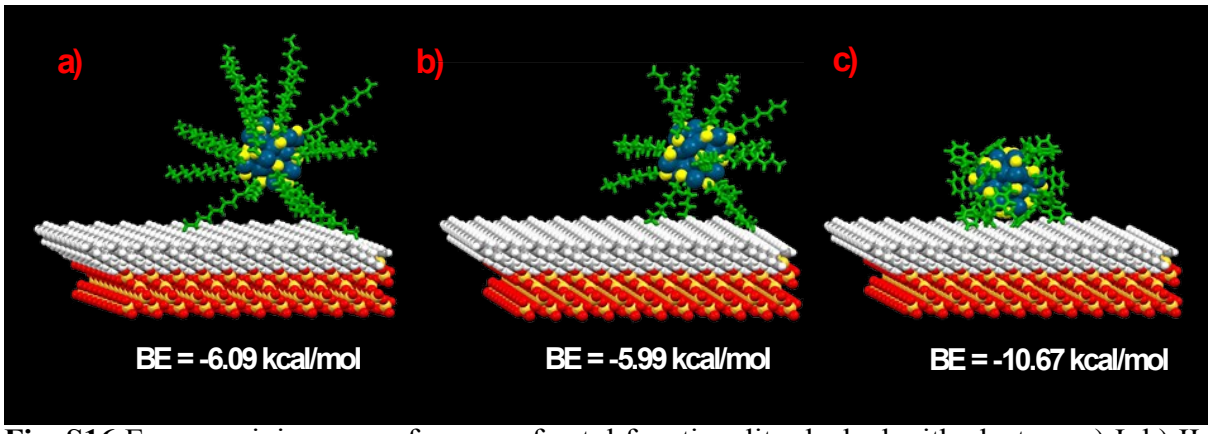

Fig. S16 Energy minimum conformers of octyl functionality docked with clusters; a) I, b) II, and c) III. Color labels: golden yellow, Si; red, O; grey, C; white, H; teal, Au; yellow, S; green, DDT, OT, and PET ligands.

Supplementary information 17

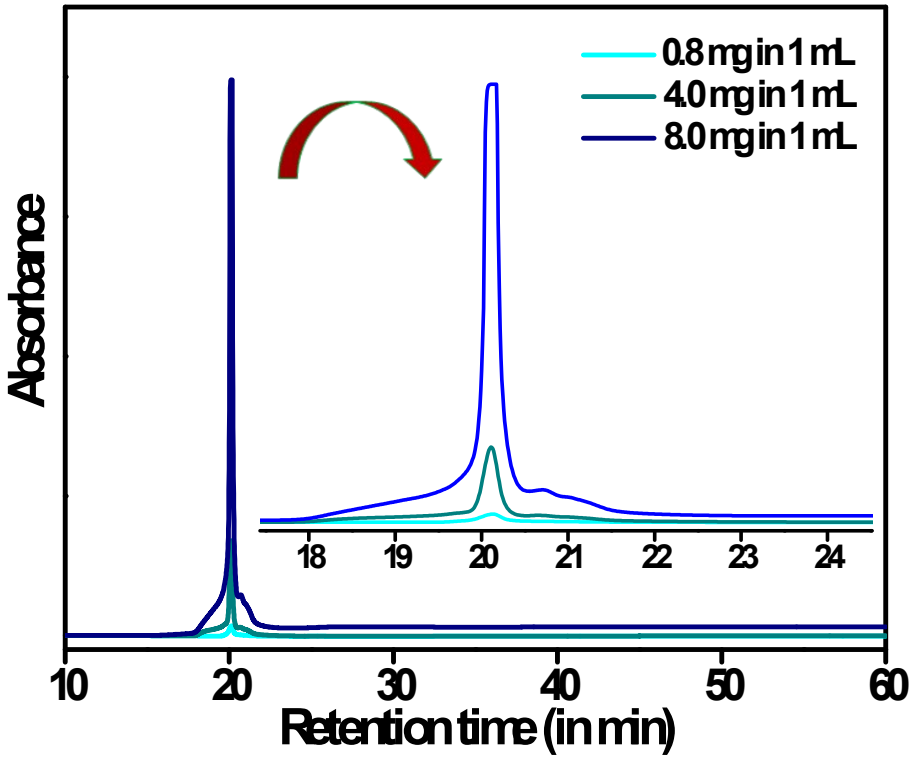

Fig. S17 Concentration-dependent chromatograms of cluster III in the phenylhexyl column at 1.0 mL/min flow rate.

Supplementary information 18

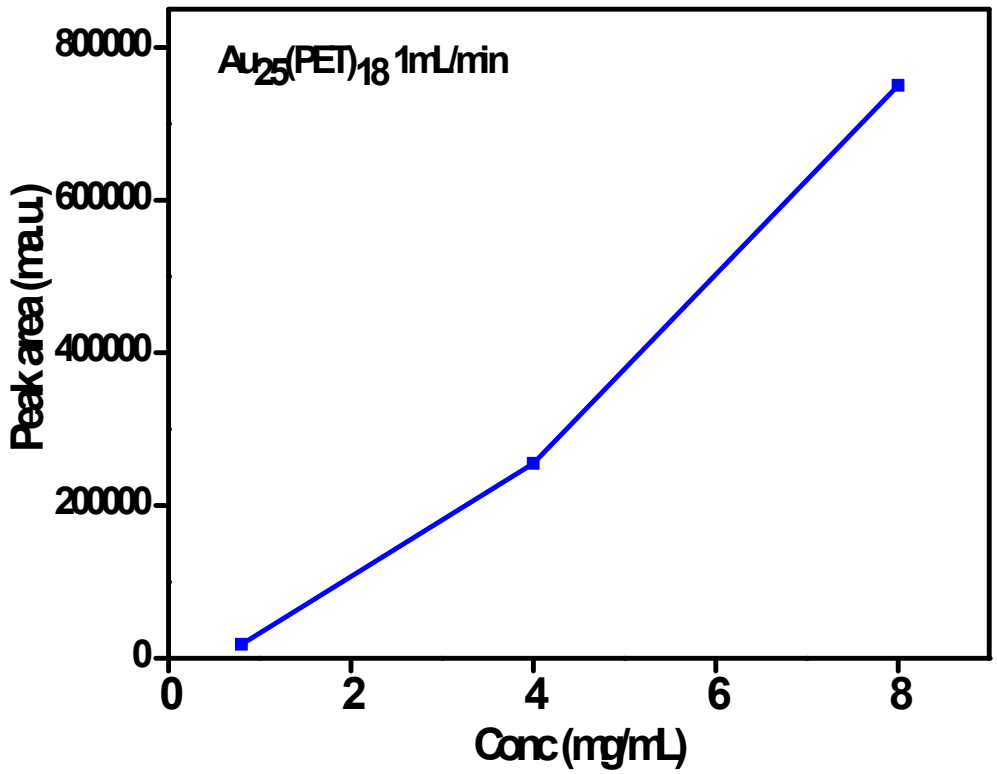

Fig. S18 Peak area vs. concentration of cluster III in the phenylhexyl column at 1.0 mL/min flow rate.

References

1. Enkovaara, J.; Rostgaard, C.; Mortensen, J. J.; Chen, J.; Dułak, M.; Ferrighi, L.; Gavnholt, J.; Glinsvad, C.; Haikola, V.; Hansen, H. A.; Kristoffersen, H. H.; Kuisma, M.; Larsen, A. H.; Lehtovaara, L.; Ljungberg, M.; Lopez-Acevedo, O.; Moses, P. G.; Ojanen, J.; Olsen, T.; Petzold, V.; Romero, N. A.; Stausholm-Møller, J.; Strange, M.; Tritsaris, G. A.; Vanin, M.; Walter, M.; Hammer, B.; Häkkinen, H.; Madsen, G. K. H.; Nieminen, R. M.; Nørskov, J. K.; Puska, M.; Rantala, T. T.; Schiøtz, J.; Thygesen, K. S.; Jacobsen, K. W., Electronic structure calculations with GPAW: a real-space implementation of the projector augmented-wave method. *Journal of Physics: Condensed Matter* **2010,** *22* (25), 253202.
2. Perdew, J. P.; Burke, K.; Ernzerhof, M., Generalized Gradient Approximation Made Simple [Phys. Rev. Lett. 77, 3865 (1996)]. *Physical Review Letters* **1997,** *78* (7), 1396-1396.
3. Larsen, A. H.; Vanin, M.; Mortensen, J. J.; Thygesen, K. S.; Jacobsen, K. W., Localized atomic basis set in the projector augmented wave method. *Physical Review B* **2009,** *80* (19), 195112.
4. Morris, G. M.; Huey, R.; Lindstrom, W.; Sanner, M. F.; Belew, R. K.; Goodsell, D. S.; Olson, A. J., AutoDock4 and AutoDockTools4: Automated docking with selective receptor flexibility. *Journal of Computational Chemistry* **2009,** *30* (16), 2785-2791.
5. Prewitt, C. T.; Weidner, D. J.; Levien, L., Structure and elastic properties of quartz at pressure. *American Mineralogist* **1980,** *65* (9-10), 920-930.
6. Hanwell, M. D.; Curtis, D. E.; Lonie, D. C.; Vandermeersch, T.; Zurek, E.; Hutchison, G. R., Avogadro: an advanced semantic chemical editor, visualization, and analysis platform. *Journal of Cheminformatics* **2012,** *4* (1), 17.